Control of Ion Beam Generation in Intense Short Pulse Laser Target Interaction

T. Nagashima[1], T. Izumiyama[1], D. Barada[1], S. Kawata[1], W. M. Wang[2]
Y. Y. Ma[3], Q. Kong[4], Y. J. Gu[1,4]

[1]*Graduate School of Engineering, Utsunomiya University*

[2]*Institute of Physics Chinese Academy of Sciences, China*

[3]*National University of Defense Technology, China*

[4]*Institute of Modern Physics, Fudan University, China*

ABSTRACT

In intense laser plasma interaction, several issues still remain to be solved for future laser particle acceleration. In this paper we focus on a control of generation of high-energy ions. In this study, near-critical density plasmas are employed and are illuminated by high intensity short laser pulses; we have successfully generated high-energy ions, and also controlled ion energy and the ion energy spectrum by multiple-stages acceleration. We performed particle-in-cell simulations in this paper. The first near-critical plasma target is illuminated by a laser pulse, and the ions accelerated are transferred to the next target. The next identical target is also illuminated by another identical laser pulse, and the ion beam introduced is further accelerated and controlled. In this study four stages are employed, and finally a few hundreds of MeV of protons are realized. A quasi-monoenergetic energy spectrum is also obtained.

Keywords

Laser ion acceleration, target plasma, post acceleration, multistage acceleration

1. Introduction

Particle accelerators have played important roles in various fields, such as basic particle physics, cancer therapy, industrial applications, inertial confinement fusion, etc. Existing accelerator has a limitation of the acceleration gradient, and its size and cost are huge.

On the other hand, intense short-pulse lasers are now available. Based on the new laser technology, new acceleration mechanisms have been proposed using the laser pulse, as alternatives of the conventional accelerator. However, there are also issues in the laser particle acceleration method. In the laser particle acceleration, the issues includes a lack of controllability for particle beam quality and for its lower energy efficiency. These issues should be addressed toward a realistic laser particle accelerator. In this study we focus a laser proton beam generation.

In the laser ion acceleration, first target electrons are kicked by the incoming intense laser pulse, and form an electron cloud at the target surfaces. The target substrate becomes positively charged, and a strong electric field is created at the target surfaces. At the target rear surface, if an ion source is located, the ions are accelerated. This ion acceleration

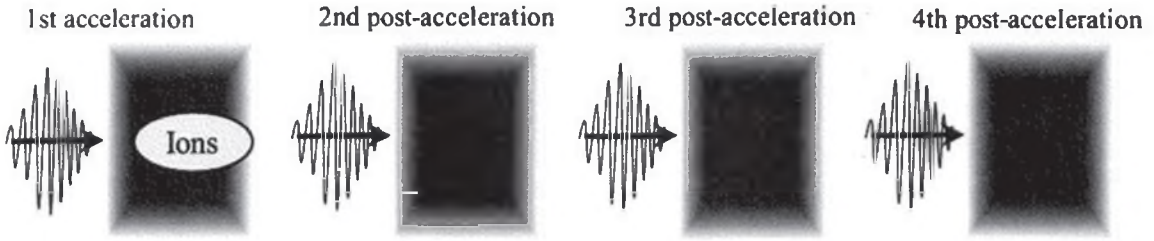

Fig. 1 Simulation model for multi-stage ion acceleration

mechanism is called as the TNSA (Target Normal Sheath Acceleration). When the target is a gas target, a laser would penetrate the gas plasma target with a lower speed than the speed of light c in vacuum. When the intense laser illuminate the gas plasma target, electrons are also accelerated and propagate in the plasma. Then the strong electron current is generated, and then a strong magnetic field is generated. At the increase phase of the strong magnetic field, an inductively generated longitudinal field is created. The inductive electric field propagates with a lower speed than c, depending on the plasma density. When the inductive electric field speed is close to the ion beam propagation speed in the plasma, the ion beam is continuously accelerated.

In this study, we perform 2.5-dimensional PIC (Particle-In-Cell) [1] simulations to improve the ion beam quality and to control the ion energy spectrum. Our simulation results demonstrate that the multi-stage ion acceleration provides a remarkable increase in the proton energy and also provides a control method of the proton energy spectrum.

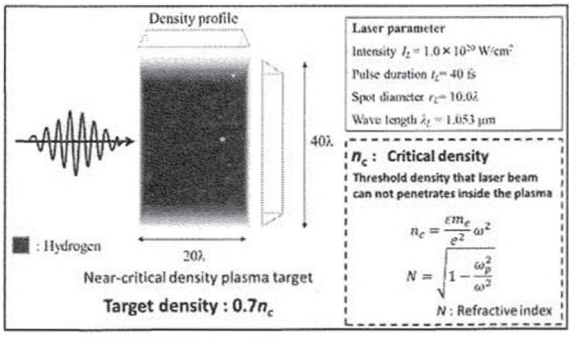

Fig. 2 Simulation target model

2. Generation of High Energy Ions Using Plasma

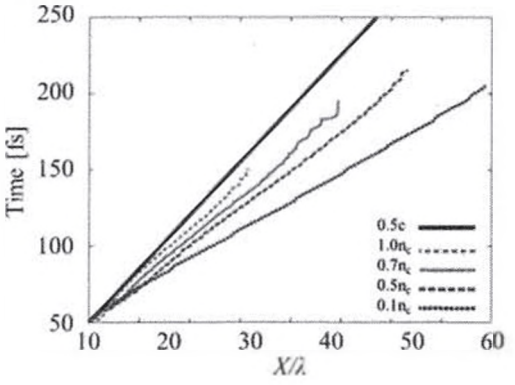

Fig. 3 Laser speed in plasma target

Figure 1 represents a simulation model for the multi-stage laser ion acceleration. The laser intensity is 1.0×10^{20}W/cm^2, the pulse length is 40fs, the spot size is 10λ, and the wavelength is $\lambda = 1.053\,\mu$m. We use a plasma target In Fig. 2 the simulation model is shown. The density of the plasma target is set to be $0.7n_c$, and the target has a linear density gradient in 0.2λ in all the directions. Here n_c shows the critical density, at which the plasma frequency is equal to the laser frequency. In this paper we employ the 4 stages for the laser proton acceleration. The huge simulation is divided into 4 simulations. Each simulation box has one target, and in each simulation box one laser illuminates the plasma target (see Fig. 2). At the 1st ion source stage, the accelerated protons reaches to the right boundary and are transferred to the next simulation. This simulation procedure is repeated.

Figure 3 shows laser speeds in various plasma densities. When the target density is $1.0n_c$, the speed of light becomes $0.501c$ in the plasma. When the

target density is $0.7n_c$, the speed of light becomes $0.624c$. At the 4th stage, our results show that the proton speed becomes $0.5c$~$0.6c$, which is generally required for cancer treatment. When the plasma density is about $0.7n_c$, the laser speed coincides with the proton speed, so that protons are continuously accelerated well. Therefore, we employ the target density of $0.7n_c$ in the simulations.

Figure 4 shows the results of the simulations for the 4 stages. The first stage is the ion source, and the other three stages are the post accelerations. We employ the same target and the same laser in all stages.

In the ion source, the maximum electric field is 16.7MV/μm at the target rear side. The electric field is the TNSA field. The energy conversion efficiency is 2.12% from the laser to the protons. The high-energy protons more than 20MeV are loaded into the 2nd post-acceleration. In the 2nd post-acceleration stage, 17.4% of the beam protons loaded have reached more than 60MeV. The energy conversion efficiency of the ion beam from the laser is 0.566%. The protons accelerated more than 60MeV in the 2nd post-acceleration are introduced to the 3nd post-acceleration. In the 3rd stage, 7.58% of the beam protons introduced have reached more than 120MeV. The energy conversion efficiency of the ion beam from the laser was 4.67×10^{-2}%. The protons more than 120MeV in the 3nd post-acceleration are introduced to the 4th post-acceleration. In the 4th stage, 5.87% of the beam protons loaded reached

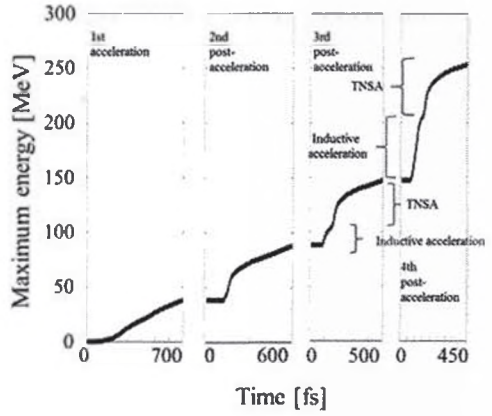

Fig. 4 Maximum ion energy history

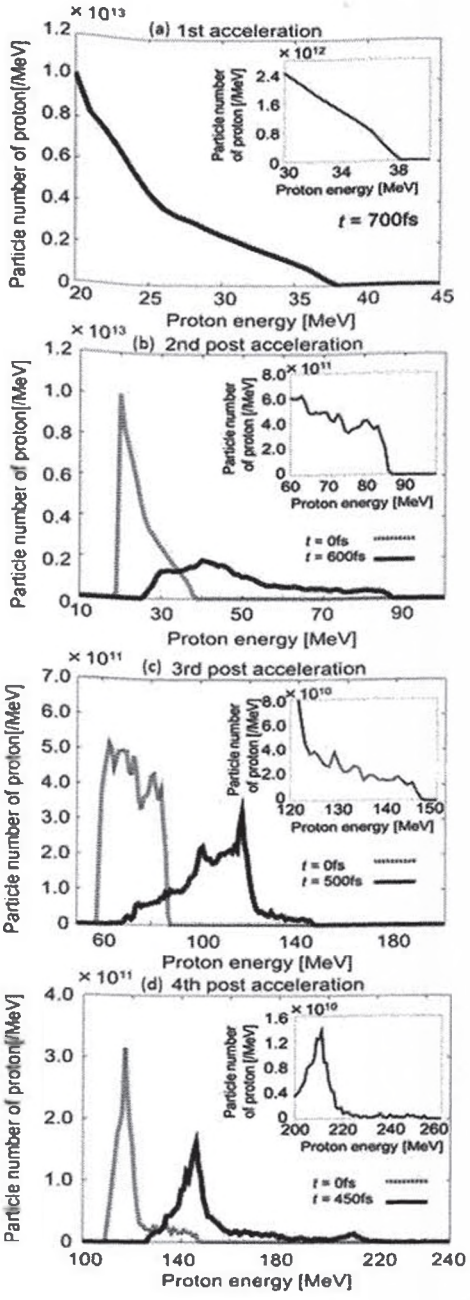

Fig. 5 Proton kinetic energy spectra. (a) 1st acceleration at 700fs, (b) 2nd post-acceleration at 0fs and 600fs, (c) 3rd post-acceleration at 0fs and 500fs, and (d) 4th post-acceleration at 0fs and 450fs

more than 200MeV. The energy conversion efficiency of the ion beam from the laser was 1.46×10^{-2} %.

In Fig. 4 the maximum energy history is presented in each stage of the 1st~4th accelerations. The

maximum energy of protons reaches 254MeV in the 4th post-acceleration.

In the 1st ion source stage and the 2nd post-acceleration stage, TNSA works mainly for the proton acceleration. In the 3rd and 4th post-acceleration, the inductive acceleration works first for the continuous proton acceleration inside the plasma target and then TNSA contributes to the further proton acceleration at the target rear surface. In the 3rd and 4th stages the speed of the induced electric field was almost identical to the ion beam speed. The velocity of ion beam is about 0.566c ~ 0.653*c*, the group velocity of the induced electric field within the plasma target is 0.548c in 4th post-acceleration.

In Figs. 5 (a)-(d) we shows the proton kinetic energy spectra in each acceleration stage. The inset figures at the upper right in each figure shows the high energy part. The actual total number of the protons more than 200MeV is about 1.39×10^{11} particles/cm. The spectrum peak of the high-energy proton group is located at about 210MeV.

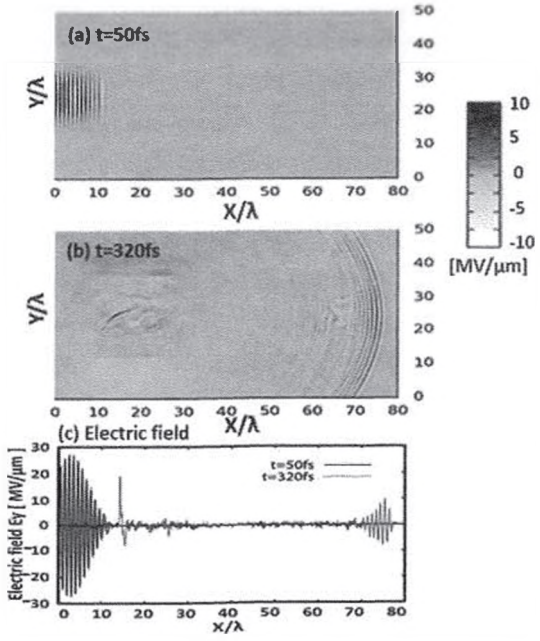

Fig. 6 Spatial distributions of the laser electric field *Ey*. (a)t=50fs, (b)t=320fs. And (c)The magnitude of the electric field *Ey* for *x* region

3. Effect of Target Debris on Multi-Stage Acceleration

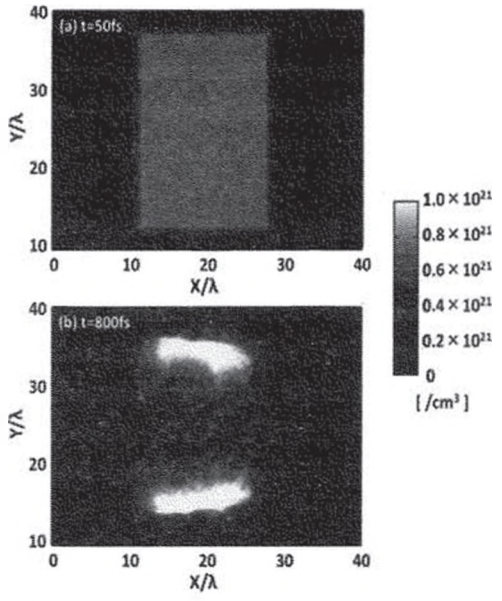

Fig. 7 Electron density of the plasma target, after the laser passed through the target

In this chapter, we investigate the afterglow effect of the first laser pulse on the second target and the effect of the first-target debris on the second laser pulse propagation and also the second target. The simulation parameters used here are the same as in Chapter 2.

First, we examine the afterglow laser field after passing through the first target. Figures 6 show the spatial distributions of the laser electric field *Ey* at 50fs (solid line) and at 320fs (dashed line). The electric field of the first transmitted laser becomes weak so that the second target is not significantly influenced.

Figures 7 show the electron density of the first plasma target, after the first laser passed through the target. Figures 7 show that the electron density around the central axis decreases well.

When the second incoming laser passes through the first target debris toward the 2nd post-acceleration, we find that the debris effect is minor. Figure 8 presents the history of the average electron density along the center axis of the target.

We also examined how much the second laser

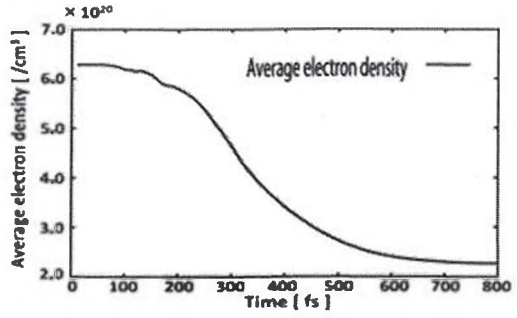

Fig. 8 Time variation of the average electron density in ($20\lambda < y < 30\lambda$, $9.5\lambda < x < 29.5\lambda$)

electric field decreases, when the second laser illuminates the second target through the first target debris. Figure 9 shows the laser electric field. The second laser does not feel any significant effect by the first target debris, except the diffraction effect.

4. Conclusions

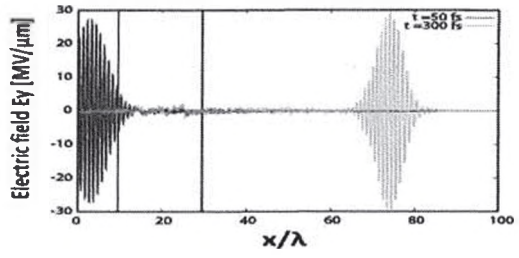

Fig. 9 Laser electric field *Ey* in *x* region at 50fs and 300fs

In this study, we focused on the intense laser proton acceleration using a near-critical gas plasma target, in which the inductive acceleration field moves with a speed less than *c*. The slower speed of the inductive acceleration field contributed to the continuous proton acceleration inside the plasma target. The TNSA also contributes to the ion acceleration in this study at the target rear surface.

In this particular study, we have focused on the improvement of the peak energy of the ion beam and also on the mono-energetic spectrum control. Our present study results demonstrated that the multi-stage acceleration realizes the high-energy of protons more than 200MeV or more and provides a tool to produce a mono-energetic proton beam. The proton energy of 200-250MeV could be used for the cancer therapy.

The laser-based multiple ion acceleration provides a new tool to control the ion energy and the ion energy spectrum. The idea of the multi-stage acceleration in the controllable manner may open a new direction of the laser particle acceleration scheme.

Acknowledgements

This study is party supported by MEXT, JSPS, CORE (Center for Optical Research and Education, Utsunomiya Univ.), ASHULA project (JSPS Asia Core to Core Program: Asian Core Program for High Energy Density Science Using Intense Laser Photons) / ILE Osaka University.

References

[1] B. F. LASINSKI, et al., "Particle-in-cell simulations of ultra intense laser pulses propagating through overdense plasma for fast-ignitor and radiography applications", *Phys. Plasmas*, **6**, 2041 (1999)

[2] I. VELCHEV, et al., "Laser-induced Coulomb mirror effect: Applications for proton acceleration", *Phys. Plasmas*, **14**, 033106 (2007)

[3] T. NAKAMURA, et al., "High-Energy Ions from Near-Critical Density Plasmas via Magnetic Vortex Acceleration", *Phys. Rev. Lett.*, **105**, 135002 (2010)

[4] M. ROTH, et al., "Fast Ignition by Intense Laser-Accelerated Proton Beams", *Phys. Rev. Lett.*, **86**, 436 (2001).

[5] M. NAKATSUTSUMI, et al., "Fast focusing of short-pulse lasers by innovative plasma optics toward extreme intensity", *Opt. Lett.*, **35**, No. 13 (2010)

[6] A. P. ROBINSON, et al ., "Effect of Target Composition on Proton Energy Spectra in Ultraintense Laser-Solid Interactions", *Phys.*

Rev. Lett., **96,** 035005 (2006)

[7] J. PSIKAL, et al., "Ion acceleration by femtosecond laser pulses in small multispecies targets", *Phys. Plasmas*, **15**, 053102 (2008)

[8] E. FOURKAL, et al., "Coulomb explosion effect and the maximum energy of protons accelerated by high-power lasers", *Phys. Rev. E.*, **71**, 036412 (2005)

[9] F. LINDAU, et al., "Laser-Accelerated Protons with Energy-Dependent Beam Direction", *Phys. Rev. Lett.*, **95**, 175002 (2005)

[10] M. NAKAMURA, et al., "Robustness of a Tailored Hole Target in Laser-Produced Collimated Proton Beam Generation", *J. Appl. Phys.*, **101**, 113305 (2007)

[11] T. NAKAMURA, et al., "High-Energy Ions from Near-Critical Density Plasma via Magnetic Vortex Acceleration", *Phys. Rev. Lett.*, **105**, 135002 (2010).

[12] Y. J. GU, et al., "Steady plasma channel formation and particle acceleration in an interaction of an ultraintense laser with near-critical density plasma", *Phys. Plasmas*, **18**, 030704 (2011).

[13] L. WILLINGALE, et al., "Collimated Multi-MeV Ion Beams from High-Intensity Laser Interactions with Underdense Plasma", *Phys. Rev. Lett.*, **96**, 245002 (2006).

[14] S. V. BULANOV, et al., "Ion Acceleration in a Dipole Vortex in a Laser Plasma Corona", *Plasma Phys. Rep.*, **31**, 5, pp.369-381 (2005).